IEEE Access
Multidisciplinary | Rapid Review | Open Access Journal

Received August 18, 2019, accepted September 17, 2019, date of publication September 24, 2019,
date of current version December 26, 2019.

Digital Object Identifier 10.1109/ACCESS.2019.2943544

Magnetic Anomaly Detection Based on Full Connected Neural Network

SHUCHANG LIU[1], ZHUO CHEN[1], MENGCHUN PAN[1], QI ZHANG[1], ZHONGYAN LIU[1], SIWEI WANG[2], DIXIANG CHEN[1], JINGTAO HU[2], XUE PAN[1], JIAFEI HU[1], PEISEN LI[1], AND CHENGBIAO WAN[3]

[1]College of Artificial Intelligence, National University of Defense Technology, Changsha 410073, China
[2]College of Computer, National University of Defense Technology, Changsha 410073, China
[3]China Huayin Ordnance Test Center, Huayin 714200, China

Corresponding author: Qi Zhang (13873191345@163.com)

ABSTRACT Magnetic anomaly detection (MAD) has been widely used for detecting some hidden ferromagnetic objects. Orthonormal basis function (OBFs) detector is one of the most popular methods of MAD. The OBFs detector works effectively under white Gaussian noise. However, the practical geomagnetic noise is colored noise with a power spectral density of $1/f^{\alpha}$ (f is frequency and α is noise exponent), and the signal-to-noise ratio (SNR) is usually very low. In order to improve magnetic anomaly detection performance in the case of colored noise and low SNR, a novel detection method by using full connected neural network (FCN) is proposed in the paper. Firstly, the detector based on FCN is designed and two kinds of features that include the signal's statistical property and the magnetic moment's characteristics of the target are extracted and used as the input of neural network; Then, the optimal network structure with proper number of layers and nodes is obtained; Finally, the detection performance of the detector under different SNRs and orientations of target's magnetic moment is evaluated. Simulation results show that the proposed method has better performance and achieves an incremental detection probability of about 5% to 40% under colored Gaussian noise with different noise exponent than traditional method. In the end, experiments under real geomagnetic noise also verify the effectiveness of the proposed method.

INDEX TERMS Magnetic anomaly detection, orthonormal basis functions, full connected neural network, noise suppression.

I. INTRODUCTION

Ferromagnetic objects will generate magnetic anomaly field [1]–[3] that can be detected even underwater or underground. Therefore, magnetic anomaly signal has been widely utilized to detect and locate them [4]–[6]. As a passive method, MAD has some advantages, such as simple configuration, high performance, staying unrevealed and excellent antijamming capability, and it has been widely used for prospecting, vehicle tracking and detection of concealed metal objects. However, the performance and efficiency of MAD is limited by low SNR in practical application since the magnetic anomaly signal is usually buried deeply in the geomagnetic filed and external magnetic noise [7]. For example, the magnetic anomaly signal caused by a middle submarine at the distance of 600m is only about 0.2 nT, this is because that the magnetic field signal strength of a magnetic dipole decreases as the third power of range.

Many methods have been proposed to solve this problem, such as orthonormal basis functions [8], minimum entropy filter [9], and high order crossing [10]. The OBFs method decomposes magnetic anomaly signal into three orthonormal basis functions, and the squared sum of the three coefficients is used to construct the energy detector of magnetic anomaly signal. However, the performance of OBFs degrades if the target signal is contaminated by colored noise with a power spectral density of $1/f^{\alpha}$, where f is frequency and α is noise exponent [11], which is considered as more in line with the actual situation [12]. Entropy filter and high-order crossing are the methods revealing changes in the magnetic background nature, assumed that the changes are caused by the presence of a ferromagnetic target. These methods benefit from the fact that they do not need a prior assumption of the target, which result in a simpler implementation, but it is

The associate editor coordinating the review of this manuscript and approving it for publication was Fanbiao Li.

difficult to exert its performance under the condition of low SNR.

Since the magnetic anomaly detection task can be regarded as a typical case of a binary classification task [13], [14] to identify whether the target signal exists or not, the MAD method can be regarded as a classifier. And neural network (NN) has been intensively applied to classification tasks, which could be the key to solve the problem of the insufficiency of existing approaches. For instance, in speech recognition, deep neural network (DNN) matches the state-of-the-art performance in very low SNR [15]. In image denoising, full connected neural networks can increase peak signal-to-noise ratio of images [16]. The FCN method is desirable for magnetic anomaly detection, because of two potential advantages: 1) Unlike traditional methods, its detection performance does not depend heavily on the type of noise, as long as the training sample cover the real noise, the detection performance can be guaranteed; 2) it can recognize target signal at very low SNR.

Therefore, we proposed a novel detection method based on FCN, and the optimal network structure suitable for MAD is obtained. In the proposed method, two kinds of features that includes the signal's statistical property and the magnetic moment's characteristics of the target are extracted and used as the input of neural network, which then will identify whether the target signal exists or not. Due to the powerful learning and classification function of neural network, the proposed detection method has better performance for detecting magnetic objects, which makes it more attractive in practice.

II. GUIDELINES FOR MANUSCRIPT PREPARATION

The proposed method based on FCN is depicted in Fig.1. Some features are extracted from measured signal, and delivered to the neural network as inputs. In the FCN, a node receives the input signals delivered from the previous layer, and generates the output signal processed by activation function. The detection output value is set to be 1 or 0, indicating whether there exists the target signal or not.

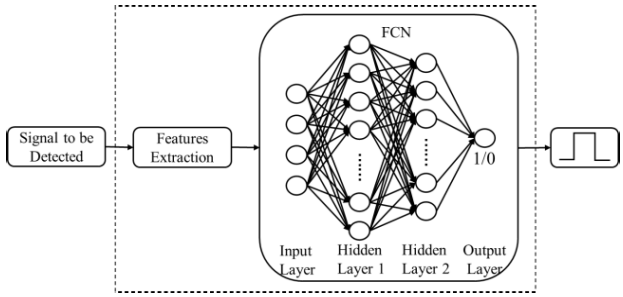

FIGURE 1. The process of the proposed method.

A. FEATURES EXTRACTION

Two different kinds of features are extracted: statistical property of the signal, and characteristics of the magnetic moment.

The variance α_0 of the signal is calculated, which is the commonly used statistical property in the data preprocessing of FCN [17]. The equation is as follows, N is the sampling points of the signal, T_r is the measured signal.

$$\alpha_0 = \frac{\sum_{i=1}^{N}\left(T_r - \sum_{i=1}^{N} T_r \Big/ N\right)^2}{N} \tag{1}$$

The three coefficients of the orthonormal basis functions are utilized as the features to characterize magnetic moment of the target. In order to obtain the coefficients, the detection model [18] is constructed as shown in Fig.2, where the target is static and the magnetometer moves parallelly to x-axis. r_0 is the closest proximity approach (CPA) from the target to the searching track of the magnetometer. And the hidden ferromagnetic target is usually regarded as a point magnetic dipole [19] in this situation.

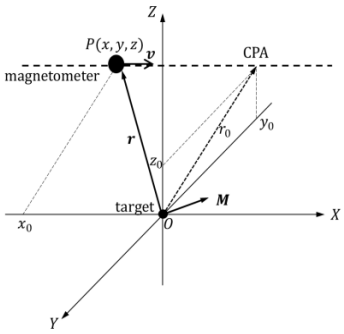

FIGURE 2. Ferromagnetic target detection model.

According to the theory of OBFs, three coefficients $\alpha_i\ (i = 1, 2, 3)$ are obtained by decomposing the measured signal T_r into a set of orthonormal basis functions:

$$T_r = \sum_{i=1}^{3} \alpha_i f_i(\tau) \tag{2}$$

where $\tau = \frac{x}{r_0}$, $f_i(\tau)\ (i = 1, 2, 3)$ is the orthonormal basis function:

$$\begin{aligned} f_1(\tau) &= \sqrt{\frac{24}{5\pi}} \frac{1 - \frac{5}{3}\tau^2}{\left[1 + \tau^2\right]^{\frac{5}{2}}} \\ f_2(\tau) &= \sqrt{\frac{128}{5\pi}} \frac{\tau}{\left[1 + \tau^2\right]^{\frac{5}{2}}} \\ f_3(\tau) &= \sqrt{\frac{128}{3\pi}} \frac{\tau^2}{\left[1 + \tau^2\right]^{\frac{5}{2}}} \end{aligned} \tag{3}$$

And the coefficient $\alpha_i\ (i = 1, 2, 3)$ of the basis function can be obtained through (4):

$$\alpha_i = \left(\frac{\mu_0 M}{4\pi r_0^3}\right)^{-1} \int_{-\infty}^{\infty} f_i(\tau)\, T_r \mathrm{d}\tau \tag{4}$$

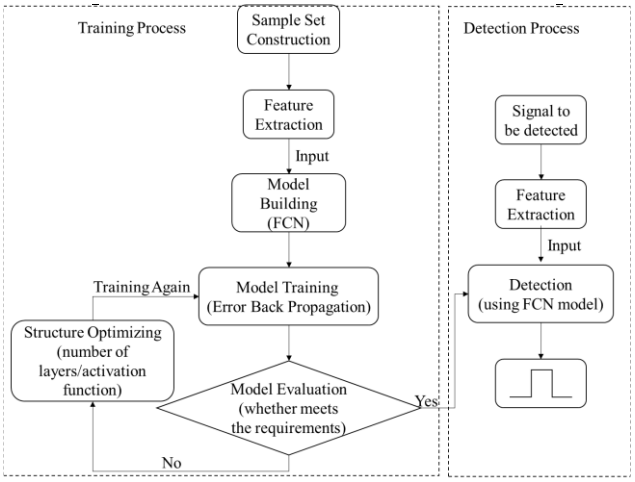

FIGURE 3. Training and detection procedure.

B. TRAINING AND DETECTION PROCEDURE

When the feature extraction is defined and clear, the training and detection flow (as shown in Fig.3) can be established and illustrated as follows:

1) DATA PREPARATION

The first step is to prepare the data. There are two operations in this step, sample data set construction and feature extraction. In the MAD sample data construction, signal and noise data are generated.

2) MODEL BUILDING

The second step is to build the model, which in this paper is FCN. As the magnetic anomaly detection task is a typical binary classification, the loss function chosen for the network is binary-crossentropy.

3) MODEL TRAINING

In this step, the model is trained with the input of data sample set.

4) MODEL EVALUATION AND FCN STRUCTURE OPTIMIZING

When the model's training process is finished, the evaluation to the model will be carried out to test whether it compliances with requirements. If the model is qualified, it can be applied to MAD; if not, some parameters of the neural network will be adjusted.

5) DETECTION TEST

The signal and noise data in test sample set are classified by the trained model. The detection performance is evaluated and compared to traditional MAD method at last step.

C. PERFORMANCE EVALUATION

The MAD problem is essentially a binary hypothesis test whether the target signal exists or not. The null hypothesis H_0 shows the latter situation, and the alternative hypothesis H_1 shows the former:

$$\begin{cases} H_0 : x = n \\ H_1 : x = s + n \end{cases} \tag{5}$$

Where x is measurement, s is signal and n is noise. The detection probability is defined to be $P_D = P_r(H_1 \mid H_1)$, and the false alarm probability to be $P_F = P_r(H_1 \mid H_0)$ [14]. Specific to the classification of FCN, whose possible results are illustrated in Table 1, the definition of the value of false alarm rate (FAR) and detection probability in this paper is shown in (6) and (7). $Num_{TP}, Num_{FN}, Num_{FP}, Num_{TN}$ are the number of TP, FN, FP, TN in the results to the sample set. To select the proper neural network, the FAR P_F of the sample set should be lower than 1.5% [20], and the detection probability P_D be higher than OBFs. If the trained model doesn't meet the requirements, the structure of the neural network will be adjusted, and network will be trained again.

$$P_F = \frac{Num_{FP}}{Num_{FP} + Num_{TN}} \tag{6}$$

$$P_D = \frac{Num_{TP}}{Num_{TP} + Num_{FN}} \tag{7}$$

TABLE 1. Four results in the binary classification task.

		Predicted Label	
		1	0
Actual Label	1	True Positive (TP)	False Negative (FN)
	0	False Positive (FP)	True Negative (TN)

III. SIMULATION AND ANALYSIS

A. DATA PREPARATION

The simulation is carried out on the basis of the magnetic anomaly detection model established in Fig.2. And the simulation parameters are set in term of real MAD situation [12], which are listed in Table 2.

TABLE 2. Simulation parameters.

Vertical component of magnetic moment	15000A $\cdot m^2$
Horizontal component of magnetic moment	62000 A $\cdot m^2$
Geomagnetic field	(35000, -2000, -33000) nT
Speed of magnetometer	100m/s
Vertical distance to target	200m
Horizontal distance to target	560m
Sampling frequency	20Hz

1) SAMPLE SET FOR FCN TRAINING

In the situation of magnetic anomaly detection, the angle between magnetic moment's orientation of target and the searching track (as shown in Fig.2) is unknown, because the target is invisible.

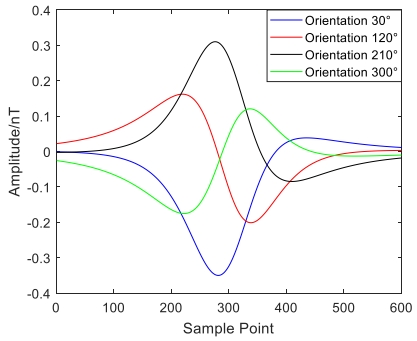

FIGURE 4. Four simulated magnetic anomaly signal waveforms of magnetic moment with different orientations.

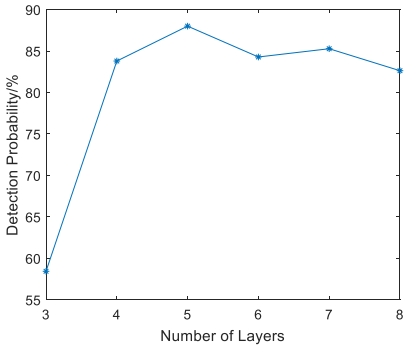

FIGURE 5. Detection probability of the detector based on FCN with different number of layers.

So as to simulate the real MAD situation and make the sample set covering as many situations as possible, the horizonal component of target's magnetic moment is rotated from 0 degree to 360 degree at the interval of 30 degree, and the vertical component remains unchanged. With each orientation of the magnetic moment, 2000 times repetitive simulations will be carried out on the magnetic anomaly signal contaminated by colored Gaussian noise (CGN) with α of a certain value. And these 12*2000 samples compose the positive sample set (with target signal). Meanwhile, 12*2000 times repetitive simulations generating CGN only are carried out to construct the negative sample set (without target signal). Fig.4 depicts the simulated magnetic anomaly signal waveforms of four typical orientation situations. It is obvious that the waveform of the signal changes when orientation of the magnetic moment varies, indicating the necessity of the sample set to cover signals in different orientations.

2) SAMPLE SET FOR TESTING GENERALIZATION ABILITY OF THE TRAINED MODEL

Although the 12 orientations above are selected to train FCN, it is hardly possible to include all conditions of angles between magnetic moment's orientation of target and the searching track. Therefore, it requires that the trained model based on 12 specific orientations has reliable generalization performance, which means the trained model can fit for as many conditions as possible.

In this case, another 12 different orientations are generated for testing generalization ability. The horizonal component of target's magnetic moment is rotated from 15 degree at the interval of 30 degree, and the vertical component remains unchanged. The simulation on each orientation is carried out 10000 times to calculate the detection probability with the trained FCN.

3) SAMPLE SET FOR TESTING THE PERFORMANCE OF THE PROPOSED MERTHOD WITH DIFFERENT CPA

In practical application of MAD, it is hard to have a prior of the distance between the target and the searching track of MAD system. Thus, position of the target is changed to test the performance of detector based on the trained FCN above with different CPA. Taking a specific orientation of magnetic moment as an example in this test (40 degree), and the horizontal distance between target and the detection system is changed as the only variable, which changes from 225m to 950m at the interval of 25m. Based on each target with different CPA, the simulation is carried out for 10000 times with target signal contaminated by CGN with different α.

TABLE 3. Structures of networks with different number of layers.

Number of Layers	Network Structure
3	4*10*1
4	4*32*10*1
5	4*32*16*10 *1
6	4*32*16*10*8*1
7	4*32*16*10*8*4*1
8	4*32*16*10*8*4*2*1

B. NETWORK STRUCTURE OPTIMIZING

Firstly, the number of layers for network is studied, which will directly affect the performance of the network. In consideration of the practical application of MAD, an optimal network should perform with high detection probability. Therefore, by using the same sample set generated as Section III.A with noise exponent α of CGN to be 0.8 and CPA to be 600m, the performances of networks are studied with different number of layers (as shown in Table 3. As Fig.5 depicts, it is obvious that the detection probability converges from four layers. According to literature [23], the neural network is better with fewer number of layers when the performances of networks are similar. Thus, in the proposed MAD task, FCN of four layers with 4*32*10*1 nodes is optimal and applied.

Secondly, activation function for input and hidden layers is studied, which is also an important parameter of neural network. There are two kinds of functions are commonly used. One is the rectified linear unit (ReLU [22]) function as (8) shows, the other is tanh function, given as (9). The former can accelerate convergence of the network in the training process, and the latter works well when the features differ significantly.

$$ReLU\,(x) = max\,(x, 0) \tag{8}$$

$$tanh\,(x) = (e^{x} - e^{-x}) \big/ \left(e^{x} + e^{-x}\right) \tag{9}$$

TABLE 4. Index of different activation functions.

	The detector based on FCN	
	ReLU	tanh
Detection Probability	83.15%	75.90%

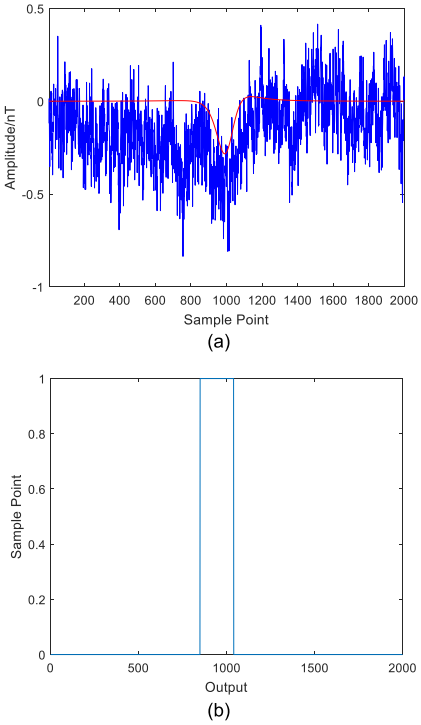

FIGURE 6. Inputs and outputs of the proposed method. (a)Simulated target signal contaminated by CGN ($\alpha = 0.8$). (b) Classification results of FCN.

Table 4 shows the detection probability for different activations, using sample data generated as Section III.A with α of CGN to be 0.8 and CPA to be 600m. Tanh function has lower detection probability than ReLU does. In this case, ReLU is better to fit the requirements of anomaly detection.

C. DETECTION PERFORMANCE COMPARISON

To evaluate and compare the performances of our proposed method with the traditional OBFs method, lots of detections were implemented to obtain the detection probabilities under different SNRs and orientations in the conditions mentioned in Section III.A. Fig.6 shows the detector's real-time response to the typical anomaly signal contaminated by noise from test samples set, in which the noise is CGN ($\alpha = 0.8$), CPA is 600m, and the orientation is 40 degree. As can be seen from Fig.6 (a), the anomaly signal is buried deeply under the noise and hard to be distinguished. Then the four features are extracted from the signal contaminated by noise, and delivered to the well-trained network. The classification results of FCN are depicted in Fig.6 (b), and it is obvious that the output is 1 when the anomaly signal exists.

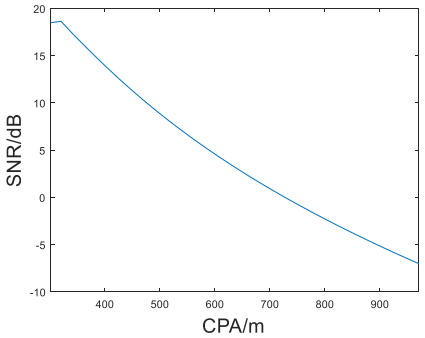

FIGURE 7. SNR of magnetic moment with different CPA.

The detection probability of different CPA is evaluated with the Monte Carlo analysis [23] and compared with traditional OBFs under different noise conditions. Since SNR decreases with the increasing of CPA as shown in Fig.7, the SNR is used to illustrate the model performance in different CPA to facilitate understanding and correspond with commonly use.

Fig.8 shows the detection probability of different SNRs under CGN with different α. Fig.8 (a) shows the detection probability with CGN ($\alpha = 0.5$), and the magnetic moment's orientation is 40 degree. It is founded that the proposed method achieves a slightly increment than OBFs in different SNRs. Fig.8 (b) shows the detection probability with CGN ($\alpha = 0.8$), and it indicates that the detection probability of the proposed method has an increase of about 5%-20% compared with the traditional OBFs in different SNRs. Fig.8 (c) shows the detection probability with CGN ($\alpha = 1$), and it is obvious that the proposed method has better performance than the traditional OBFs with an additional detection probability between 5% and 40%. These results consistently demonstrate that our proposed method has a good performance under CGN with different noise exponent α, and the improvement is more evident when α increases.

In addition, the detection probability of different orientations is also evaluated and compared with the traditional OBFs. Taking CPA = 600m as an example, the detection probabilities of different orientations are tested. Similarly, the evaluation process is fully consistent with the above. Fig.9 (a)∼(c) show the detection probability of different orientations under CGN with different noise exponent α. It is obvious that the proposed method has a better detection probability under different orientations than the traditional OBFs.

IV. EXPERIMENT

A. EXPERIMENT SYSTEM

To further evaluate our proposed method, a scheme including simulation and experimentation is designed. The real-world magnetic noise is acquired by a magnetic measurement system in suburban areas, where the ambient magnetic activity due to external sources, such as power lines and traffic, is very low. As shown in Fig.10, the measurement system mainly

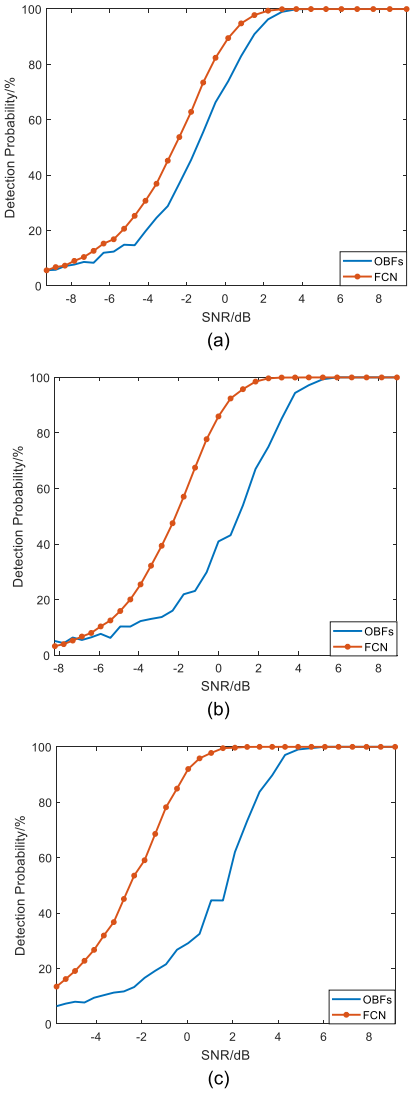

FIGURE 8. Detection probability of two methods with different noise. (a) Detection probability of two methods with CGN ($\alpha = 0.5$), (b) Detection probability of two methods with CGN ($\alpha = 0.8$), (c) Detection probability of two methods with CGN ($\alpha = 1$).

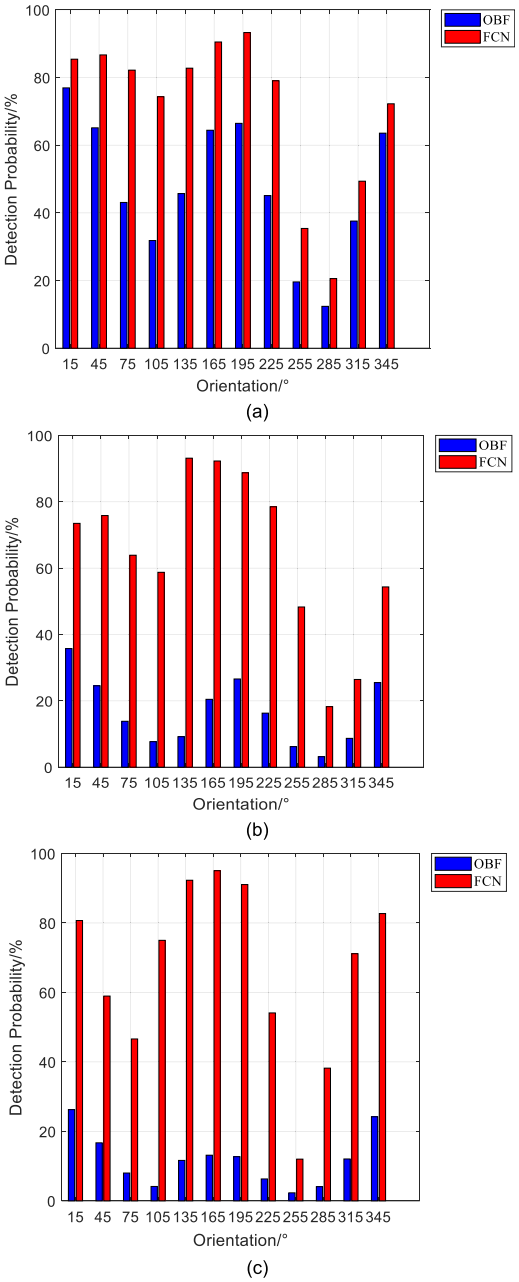

FIGURE 9. Detection probability of two methods with different orientation of target magnetic moment. (a) Detection probability of two methods with CGN ($\alpha = 0.5$), (b) Detection probability of two methods with CGN ($\alpha = 0.8$), (c) Detection probability of two methods with CGN ($\alpha = 1$).

contains magnetic sensor and data acquisition and processing devices are controlled by PC computer. the magnetometer has an intrinsic noise of $< 50\ \mathrm{pT}/\sqrt{\mathrm{Hz}}$ at 1 Hz [24], and its output was sampled with a sampling period Ts of 0.05 s. And the typical magnetic anomaly signal is generated by simulation.

B. GEOMAGNETIC NOISE MODEL

Fig.11 shows a typical segment of 10,000 readings from the acquired magnetic noise, which mainly consists of external geomagnetic noise and intrinsic sensor noise.

Fig.12 (a) shows the normalized histogram of the recordings after detrending. The skewness of the recordings after detrending is 0.05, the kurtosis is 3.31 and the STD is 0.16 nT, and the histogram of measured noise resembles a PDF of Gaussian distribution. Considering that the skewness of a Gaussian random variable is 0 and its kurtosis is 3, the geomagnetic noise can be treated as Gaussian noise. Fig.12 (b) shows the PSD of typical recorded geomagnetic field after detrending, which is related to $1/f^{\alpha}$, as a result of the geomagnetic pulsations and other interferences. It is calculated that the noise exponent is about 0.8, which means that magnetic anomaly signa is actually contaminated by colored noise.

C. TEST RESULTS WITH REAL-WORLD MAGNETIC NOISE

After acquiring the real geomagnetic noise, the trained sample set is constructed according to the synthesis method

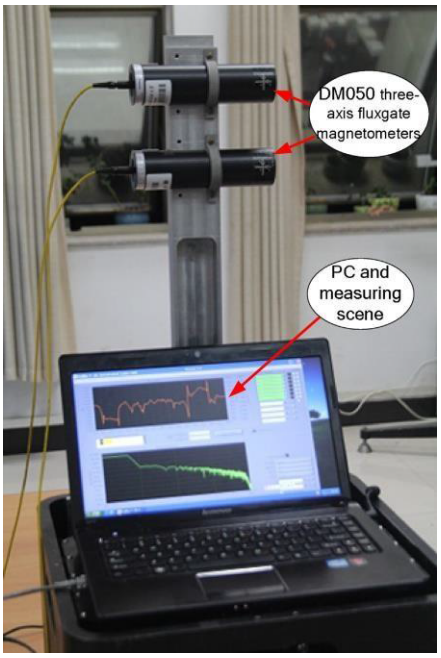

FIGURE 10. The magnetic measurement system.

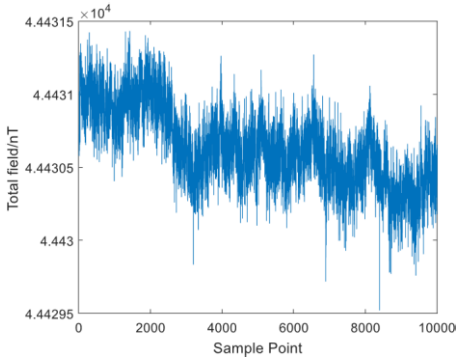

FIGURE 11. Readings of real magnetic noise.

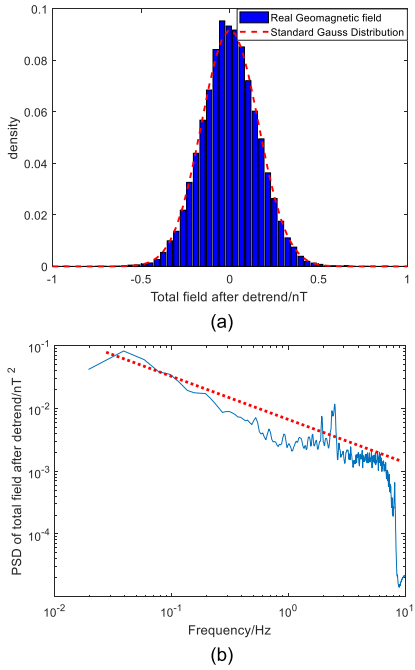

FIGURE 12. Characteristic of the recordings after detrending. (a)Normalized histogram, (b)PSD.

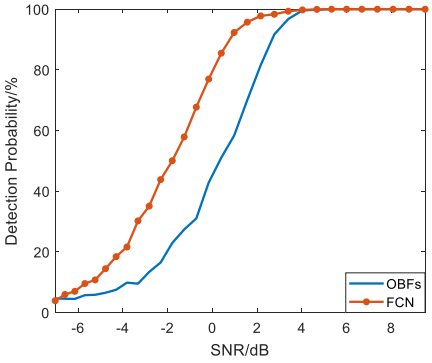

FIGURE 13. Detection probability of two methods with real magnetic noise.

mentioned in Section III.A, and it will be used as the training input of neural network. In the detection procedure, the synthesis signal contaminated by real noise is regarded as the input of detector, the performance between our proposed method and traditional method is tested and compared. It should be noted that each repetition is implemented by using the same synthesis anomaly signal but different noise samples from the measurements.

The detection results of two methods are drawn and compared in Fig.13. It is indicated that the proposed method has an incremental detection probability between 5% and 20% in different SNRs. The experiment results are in accordance with the results of previous simulation on CGN ($\alpha = 0.8$), so it is clarified that our proposed method worked well in practice, and provided better detection performance than the traditional method.

V. CONCLUSION

In this paper, we proposed an effective method of magnetic anomaly detection method based on full connected neural network. Firstly, we introduced the detection theory, then the optimal network structure with layers is obtained, finally we evaluated the detector's performance for detecting the anomaly signal embedded in noise under different SNRs and orientations. Results on simulated and real magnetic noise indicate that the proposed method has higher detection probability than traditional OBFs method. Future work will concentrate on utilizing the raw data of magnetic anomaly signal and noise to improve the detection performance furtherly.

REFERENCES

[1] T. R. Clem, "Progress in magnetic sensor technology for sea mine detection," *Proc. SPIE*, vol. 3079, pp. 354–371, Jul. 1997.

[2] A. Sheinker, B. Lerner, N. Salomonski, B. Ginzburg, L. Frumkis, and B.-Z. Kaplan, "Localization and magnetic moment estimation of a ferromagnetic target by simulated annealing," *Meas. Sci. Technol.*, vol. 18, no. 11, pp. 3451–3457, 2007.

[3] W. Eyal, G. Boris, and C. Tsuriel, "High resolution marine magnetic survey of shallow water littoral area," *Sensors*, vol. 7, no. 9, pp. 1697–1712, Sep. 2007.

[4] D. Liu, X. Xu, W. Zhu, X. Liu, G. Yu, G. Fang, and C. Fei, "Direction identification of a moving ferromagnetic object by magnetic anomaly," *Sens. Actuators A, Phys.*, vol. 229, pp. 147–153, Jun. 2015.

[5] Y. Huang and Y.-L. Hao, "Method of separating dipole magnetic anomaly from geomagnetic field and application in underwater vehicle localization," in *Proc. IEEE Int. Conf. Inf. Autom.*, Jun. 2010, pp. 1357–1362.

[6] L. V. Eppelbaum, "Study of magnetic anomalies over archaeological targets in urban environments," *Phys. Chem. Earth*, vol. 36, no. 16, pp. 1318–1330, Feb. 2011.

[7] D. Liu, X. Xu, and C. Huang, "Adaptive cancellation of geomagnetic background noise for magnetic anomaly detection using coherence," *Meas. Sci. Technol.*, vol. 26, no. 1, pp. 015008-1–015008-6, Dec. 2015.

[8] B. Ginzburg, L. Frumkis, and B. Z. Kaplan, "Processing of magnetic scalar gradiometer signals using orthonormalized functions," *Sens. Actuators A, Phys.*, vol. 102, nos. 1–2, pp. 67–75, Dec. 2002.

[9] A. Sheinker, B. Ginzburg, N. Salomonski, P. A. Dickstein, L. Frumkis, and B. Z. Kaplan, "Magnetic anomaly detection using high-order crossing method," *IEEE Trans. Geosci. Remote Sens.*, vol. 50, no. 4, pp. 1095–1103, Apr. 2012.

[10] A. Sheinker, N. Salomonski, B. Ginzburg, L. Frumkis, and B.-Z. Kaplan, "Magnetic anomaly detection using entropy filter," *Meas. Sci. Technol.*, vol. 19, no. 4, pp. 045205-1–045205-5, Feb. 2008.

[11] A. Sheinker, A. Shkalim, B. Ginzburg, L. Frumkis, B.-Z. Kaplan, and N. Salomonski, "Processing of a scalar magnetometer signal contaminated by $1/f^{\alpha}$ noise," *Sens. Actuators A, Phys.*, vol. 138, pp. 105–111, Jul. 2007.

[12] S. M. Kay, *Fundamentals of Statistical Signal Processing: Detection Theory*. Englewood Cliffs, NJ, USA: Prentice-Hall, 1998, pp. 61–75.

[13] H. V. Poor, *An Introduction to Signal Detection and Estimation*. New York, NY, USA: Springer-Verlag, 1994.

[14] S. Zozor, L.-L. Rouve, J.-L. Coulomb, H. Henocq, and G. Cauffet, "Compared performances of MF-based and locally optimal-based magnetic anomaly detection," in *Proc. IEEE Eur. Signal Process. Conf.*, Aug. 2010, pp. 149–153.

[15] M. L. Seltzer, D. Yu, and Y. Wang, "An investigation of deep neural networks for noise robust speech recognition," in *Proc. IEEE Int. Conf. Acoust., Speech Signal Process. (ICASSP)*, May 2013, pp. 7398–7402.

[16] H. C. Burger, C. J. Schuler, and S. Harmeling, "Image denoising: Can plain neural networks compete with BM3D?" in *Proc. IEEE Conf. Comput. Vis. Pattern Recognit. (CVPR)*, Jun. 2012, pp. 2392–2395.

[17] M. T. Hagan, H. B. Demuth, and M. H. Beale, *Neural Network Design*. Beijing, China: China Machine Press, 2002.

[18] C. Wan, M. Pan, Q. Zhang, D. Chen, H. Pang, and X. Zhu, "Performance improvement of magnetic anomaly detector using Karhunen–Loeve expansion," *IET Sci., Meas. Technol.*, vol. 11, no. 5, pp. 600–606, May 2017.

[19] Z. Liu, H. Pang, M. Pan, and C. Wan, "Calibration and compensation of geomagnetic vector measurement system and improvement of magnetic anomaly detection," *IEEE Geosci. Remote Sens. Lett.*, vol. 13, no. 3, pp. 447–451, Mar. 2016.

[20] R. N. Forrest, "A program to compute magnetic anomaly detection probabilities. Revision 2," Naval Postgraduate School, Monterey, CA, USA, Tech. Rep., 1988.

[21] Y. C. Ho and D. L. Pepyne, "Simple explanation of the no-free-lunch theorem and its implications," *J. Optim. Theory Appl.*, vol. 3, no. 115, pp. 549–570, 2002.

[22] X. Glorot, A. Bordes, and Y. Bengio, "Deep sparse rectifier neural networks," in *Proc. 14th Int. Conf. Artif. Intell. Statist. (AISTATS)*, vol. 15, Jan. 2010, pp. 315–323.

[23] K. Mosegaard and M. Sambridge, "Monte Carlo analysis of inverse problems," *Inverse Problems*, vol. 18, no. 3, pp. R29–R54, Apr. 2002.

[24] STL. (2008). *DM050 Handbook*. [Online]. Available: https://www.stl-gmbh.de

SHUCHANG LIU is currently pursuing the degree with the National University of Defense Technology (NUDT), China. Her current research interests include magnetic anomaly detection and neural network.

ZHUO CHEN is currently pursuing the Ph.D. degree with the National University of Defense Technology (NUDT), China. His current research interest includes geomagnetic navigation.

MENGCHUN PAN received the Ph.D. degree from the National University of Defense Technology (NUDT), China, where he is currently a Professor with the College of Artificial Intelligence. His current research interests include electromagnetic testing and instrumental science and technology.

QI ZHANG received the Ph.D. degree from the National University of Defense Technology (NUDT), China, where he is currently an Associate Professor with the College of Artificial Intelligence. His current research interests include magnetic anomaly detection, magnetometer calibration, and electromagnetic testing.

ZHONGYAN LIU received the Ph.D. degree from the National University of Defense Technology (NUDT), China, where he is currently a Research Associate with the College of Artificial Intelligence. His current research interests include geosciences research, digital signal processing, magnetic object detection, and instrumental science and technology.

SIWEI WANG is currently pursuing the degree with the National University of Defense Technology (NUDT), China. His current research interests include kernel learning, unsupervised multiple-view learning, scalable kernel k-means, and deep neutral network.

DIXIANG CHEN received the Ph.D. degree from the National University of Defense Technology (NUDT), China, where he is currently a Professor with the College of Artificial Intelligence. His current research interests include advanced test systems, intelligent instruments, and nondestructive testing.

JINGTAO HU is currently pursuing the degree with the National University of Defense Technology (NUDT), China. Her current research interests include unsupervised abnormal detection, outlier detection, and neutral network.

XUE PAN is currently pursuing the degree with the National University of Defense Technology (NUDT), China. His current research interests include geomagnetic navigation and geomagnetic calibration.

JIAFEI HU received the Ph.D. degree from the National University of Defense Technology (NUDT), China, where he is currently an Associate Researcher with the College of Artificial Intelligence. His current research interests include modulated magnetoresistive sensors, MEMS, and 1/f noise suppression.

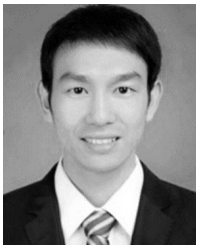

PEISEN LI received the Ph.D. degree from Tsinghua University (THU), China. He is currently a Lecturer of the College of Artificial Intelligence, National University of Defense Technology (NUDT), China. His current research interests include spin electric devices and the application of magnetic sensors.

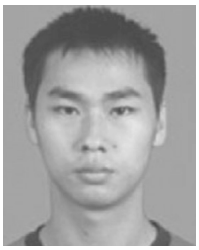

CHENGBIAO WAN received the Ph.D. degree from the National University of Defense Technology (NUDT), China. He is currently an Engineer of the China Huayin Ordnance Test Center, China. His current research interests include instrumental science and technology.